

# Least Squares Support Vector Machine Approach for Predicting Frictional Performance of Industrial Brake Pad Materials

N.S.M. Eltayb<sup>1</sup> and Abeer Hamdy<sup>2</sup>

<sup>1</sup>British University in Egypt, Elshorouk City, Egypt

<sup>2</sup>British University in Egypt, Electronics Research Institute, Egypt

E-mail: Nabil.eltayeb@bue.edu.eg; abeer.hamdy@bue.edu.eg

**Abstract**—Modeling the frictional performance of a brake pad material is difficult and requires the use of complex numerical models. The current work utilizes one of the Artificial Intelligence techniques, least squares support vector machine (LS-SVM), to model the nonlinear relationships between the input braking conditions and the frictional and thermal performance of previously developed noncommercial brake pad materials. Experimental data were produced and used in training and testing the proposed LS-SVM models. The results indicate that LS-SVM constitutes a robust methodology and the proposed models could be used to predict the friction coefficients and the induced interface temperature of brake pad materials in order to reduce experimental time and cost.

**Index Terms**—Support vector machine, regression, friction performance, brake pad materials, material informatics, machine learning.

## I. INTRODUCTION

In automotive braking systems, brake pads slow down the car's speed by transforming kinetic energy into frictional heat at the interface between the brake pad and the rotor disc. Whenever a brake-related problem arises, brake pads are always to blame. This is because brake pads appear to be more vulnerable to severe braking conditions, such as pedal pressure, vehicle speed, and disc temperature, as well as dry and wet environmental conditions [11]. Accordingly, frictional brake pad materials should maintain a relatively high, stable, and reliable friction coefficient at a wide range of braking conditions, irrespective of temperature, humidity, age, and degree of wear and corrosion, among others. Frictional performance and temperature are commonly evaluated through expensive and time-consuming experiments. In other words, this process requires developing frictional materials, selecting a test setup, conducting experiments, and evaluating the results. Therefore, researchers nowadays rely on alternative approaches, such as numerical modeling methods, to minimize the time consumption and cost. However, modeling the frictional

properties of brake pad materials is difficult and requires the use of complex numerical models.

Recently, machine learning techniques have been used as a powerful technique in the field of material science for modeling complex nonlinear relationships. These techniques were utilized to predict the tribological properties of some materials when they are exposed to various conditions, such as different heat conditions and load. In addition, they were used in guiding the development of new composite materials with previously specified mechanical properties.

Artificial neural networks (ANNs) are one of the popular machine learning techniques that have been used in the field of material science. Leifer [18] trained an ANN to predict the pit depth of aluminum alloy 1100 when subjected to natural water corrosion. In [12, 13, 19], ANN, genetic algorithm-ANN (GA-ANN), and fuzzy ANN models were trained to predict the fatigue performance of pre-corroded specimens of aluminum alloys. Rathod [23] used ANNs to predict the tribological behavior of cast Al6061-Si<sub>3</sub>N<sub>4</sub> composites. The cast composites were developed by the stir casting method and its tribological behavior was experimentally evaluated using a pin-on-disc tribometer adopting loads and sliding velocities in the ranges of 20–100 N and 0.314–1.5740 m/s, respectively. The predictions of friction coefficients and wear rates of cast composites by ANNs were very close to the experimental data. Grzegorzec [15] used feed-forward back propagation ANNs to predict the friction coefficient in disk brakes using different material compositions subjected to different conditions. Aleksendri [1] used the GA-ANN to stabilize and optimize the brake performance during a braking cycle by controlling the brake hydraulic pressure level. The ANN predicts the braking torque at the change of the brake actuation pressure, whereas the GA is used for the optimization of the brake actuation pressure in order to obtain the desired level of braking torque.

Support vector machines (SVMs) are another machine learning technique that is currently dominating ANNs and is widely used in classification and regression. SVMs provide a global solution and are less prone to overfitting, whereas ANNs can suffer from multiple local minima.

---

Manuscript received January 11, 2018; revised March 9, 2018.

SVMs were first introduced by Vapnik [29] to solve binary classification problems, and then they were extended to nonlinear regression problems. SVMs are based on structural risk minimization, unlike ANNs that are based on empirical risk minimization, and they use a nonlinear mapping to transform the input data into a multidimensional feature space. After this transformation, the SVM finds the best hyperplane inside the feature space. The nonlinear mapping depends on the so-called kernel function.

Ampazis [2] utilized SVMs to predict the degradation of the mechanical properties, due to surface corrosion, of the Al2024-t3 aluminum alloy used in the aircraft industry. Fang [14] used least squares support vector machine (LS-SVM) in simulating and monitoring the aging process of Al-Zn-Mg-Cu series alloys. Abuomar [3] used SVMs to analyze and classify a large dataset of vapor-grown carbon nanofiber/vinyl ester nanocomposites into three classes of desired mechanical properties, which are high storage modulus, high true ultimate strength, and high flexural modulus. Hou [16] trained SVMs to model the relationships between the heat treatment (heating temperature and heating period) and the mechanical properties of Tc4alloy (i.e., tensile strength, yield strength, and elongation). The accuracy of the SVM model reached 95%. Dong [8] used SVMs and ANNs to model the complex relationship between geological factors and mechanical behaviors of rocks. The results showed that the SVM model outperforms the ANN model. Martinsa [20] developed three models based on multiple regression (MR), ANN, and SVM to predict the mechanical properties (uniaxial compressive strength and deformation modulus) of Oporto granite. The SVM model showed the most accurate prediction results.

The objective of this paper is to develop two independent models for one of the previously developed noncommercial brake pad materials, based on the LS-SVM technique. The first model will represent the relationship between the input braking conditions and the friction force, whereas the second model will represent the relationship between the input braking conditions and the induced interface temperature. The developed models should be able to predict the frictional behavior of the material with minimum cost and time.

This paper is organized as follows. Section 2 discusses the methodology, which includes the process of developing the noncommercial materials, the testing experiments to gather the dataset required to train the proposed models, and the training process of the LS-SVM models. Section 3 discusses the results. Finally, Section 4 concludes the paper.

## II. METHODOLOGY

### A. Material Experiments and Data Gathering

#### 1) Frictional Materials

A great deal of effort has been made to improve the friction performance of brake rotors, including the development of nonferrous materials such as copper alloys, aluminum metal matrix composites, and carbon composites as new candidates. However, gray cast iron materials are still commonly used to fabricate frictional

brake rotor discs because of their excellent damping capacity, high thermal conductivity, and, in particular, low cost and relative ease of casting and machining [10, 11]. Thus, gray cast iron (GCI) of Flocast 4E grade was chosen as the rotor disc used in the experiments [11]. The chemical composition of the GCI rotor disc is given in Table I.

TABLE I. CHEMICAL COMPOSITION (VOL.%) OF GCI.

Material										
	C	Si	Mn	S	Cr	Cu	P	Mo	Ti	Fe
GCI	3.0-3.8	1.8-2.2	0.2-0.4	0.04 max	0.01	0.01	0.07	0.01	0.15-0.25	Bal

Brake pad materials are usually fabricated from a phenolic resin binder with the addition of mineral fibers, fillers, friction modifiers, abrasives, and metallic particles to modify the heat flow characteristics [11]. In previous work [11], four different base matrices of noncommercial materials (NF1, NF2, NF4, and NF5) were designed and manufactured, that is, non-asbestos semimetallic materials containing ten different ingredients. These ingredients comprise fiber reinforcements, binders, friction modifiers, solid lubricants, abrasives, and fillers. The relative amounts and types of these ingredients are given in Table II. The noncommercial frictional materials were manufactured by dry mixing, preforming, hot press molding at 2,500 psi and 180 °C, postcuring, and heat treatment. All noncommercial frictional materials were manufactured at CL Industries Sdn. Bhd. for brake pad manufacturing, Malaysia.

#### 2) Preparation of Specimens

In the literature, numerous test methods have been developed for evaluating friction brake pad materials. These methods range from small coupon rub tests to full-sized vehicles, on the road tests.. For this work, specimens of size 9.5 mm × 9.5 mm × 20 mm were machined from noncommercial brake pad plates of size 250 mm × 250 mm × 20 mm by Mazak CNC milling machine (Fig. 1).

TABLE II. THE INGREDIENTS OF THE NONCOMMERCIAL FRICTION BRAKE PAD MATERIALS (VOL.%).

Raw materials	Sample code			
	NF1	NF2	NF4	NF5
Metal fiber				
Steel fiber	15	20	15	20
Friction modifiers				
Brass	6	6	6	6
Cashew dust	10	10	10	10
Solid lubricant				
Graphite (C)	8	8	8	8
Abrasive				
Zircon (ZrSiO <sub>4</sub> )	3	3	3	3
Binder (matrix)				
Phenolic resin	20	15	20	15
Rubber (SBR)	-	-	10	10
Organic fiber				
Aramid pulp	10	10	-	-
Fillers, reinforcements				
CaCO <sub>3</sub>	8	8	8	8
BaSO <sub>4</sub>	20	20	20	20

Fig. 2 shows the microstructure of the polished cross section of the developed noncommercial friction brake pad material. The complexity of this proprietary friction material is clearly visible in the mixture of shiny metallic constituents and nonmetallic particles within a polymeric binder. From the figure, it is clear that NF2 and NF5 show a relatively higher percentage of steel and brass elements (shining elements), whereas NF1 and NF4 contain a high percentage (20%) of phenolic resin (dark phases).

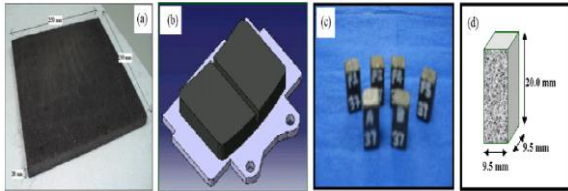


Figure 1. Friction brake pad materials [11]: (a) noncommercial brake pad material, (b) commercial brake pad, (c) the prepared brake pad specimens, and (d) specimen's dimensions.

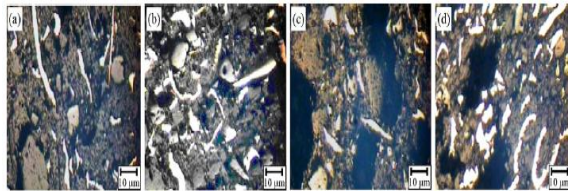


Figure 2. Microstructure of frictional materials [11]: (a) NF1, (b) NF2, (c) NF4, and (d) NF5.

### 3) Friction Test Procedure

A small-scale tribotester is designed to work at a low and moderate brake nominal pressure (up to 2.22 MPa) and speed (up to 2.1 m/s). These braking conditions were chosen to simulate the brake applications needed to maintain a specimen and the rotor disc.

### 4) Temperature Measurements

The rotor disc's temperature was measured during dry tests using a noncontact infrared (IR) thermometer (Infrared Thermometer SUMMITTM SIR10B series, accuracy:  $\pm 2\%$  of reading). The infrared thermometer was placed approximately 8 cm away from the trailing edge of the friction material (specimen), focusing on the rotor disc as illustrated in Fig. 3. Prior to the actual test, the IR thermometer was calibrated by heating up the counter face and using a surface thermocouple. However, the emissivity of the cast iron was changed because of a transfer film that developed on the wear track, and hence the accuracy of IR temperature should be considered as approximate. Besides that, the IR thermometer could not be relied on during wet tests.

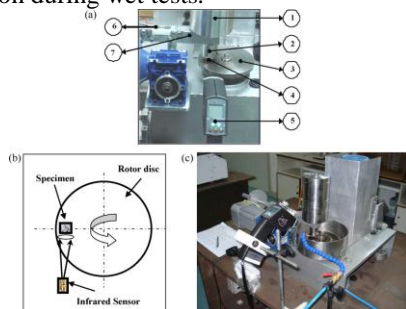


Figure 3. Braking test setup [11]: (1) dead weight, (2) specimen holder, (3) counter face, (4) pad specimen, (5) IR thermometer, (6) strain gauge, and (7) load level.

## B. The Proposed LS-SVM Models

For each of the noncommercial brake pad materials (NF1, NF2, NF4, and NF5), two independent LS-SVM models should be developed: one to predict the friction force in newton (N) and the other to predict the induced interface temperature. The inputs to each model are the braking conditions, which are the load (N), speed (rpm), and duration (s). The following subsections discuss the development process of the proposed models.

### 1) LS-SVM mathematics

LS-SVM is a variant of SVM that was proposed by Suykens and Vandewalle in 1999 [26, 27]. In LS-SVM, the solution is found by solving a set of linear equations, instead of a convex quadratic programming (QP) problem for classical SVMs. Considering a regression problem with training set  $D = \{(x_i, y_i)\}$ ,  $i = 1$  to  $n$ , where  $x_i \in R^n$  is the input pattern and  $y_i \in R$  is the corresponding output. LS-SVM solves the following optimization problem:

$$\min_{w,b,e} = \frac{1}{2} w^T w + \gamma \frac{1}{2} \sum_{i=1}^n e_i^2,$$

subject to the equality constraints

$$y_i = [w^T \varphi(x_i) + b] + e_i, \quad i = 1, \dots, n,$$

where  $\varphi(x_i)$  is a nonlinear mapping that maps the input data into a high-dimensional feature space (it is called kernel function);  $\gamma$  is the positive regularization factor that balances the trade-off between the fitting error and model complexity; parameter  $e_i$  is the model prediction error.

By introducing the Lagrangian function and differentiating it, LS-SVM can be described as follows:

$$\begin{bmatrix} K + \frac{1}{\gamma} I & 1_N \\ 1_N^T & 0 \end{bmatrix} \begin{bmatrix} \alpha \\ b \end{bmatrix} = \begin{bmatrix} Y \\ 0 \end{bmatrix},$$

where  $\alpha = (\alpha_1, \alpha_2, \dots, \alpha_N)^T$  is a vector of Lagrange multipliers,  $1_N^T = [1, \dots, 1]^T$ ,  $Y = [y_1, y_2, \dots, y_N]^T$ ,  $I$  is an  $N \times N$  identity matrix, and  $K$  is a kernel matrix with  $K(x_i, x_j) = \varphi(x_i)^T \varphi(x_j)$ .

The resulting LS-SVM model for regression becomes

$$f(x) = \sum_{i=1}^N \alpha_i^* K(x_i, x) + b^*,$$

where  $\alpha^*$  and  $b^*$  are the solutions to Eq. (2) and  $\alpha$  is proportional to the error vector  $e$  at the training patterns.

Model selection is an important issue in LS-SVM research. It involves the selection of the kernel function  $\varphi(x_i)$  and the associated kernel parameters and the selection of the regularization parameter  $\gamma$ .

Kernels used in this paper are polynomial and radial basis function (RBF). They are defined by the following equations:

*Polynomial kernel:*

$$\varphi(x_j, x_i) = (x_j^T x_i + t)^d \quad t \geq 0,$$

where  $t$  is the intercept and  $d$  is the degree of the polynomial.

*RBF kernel:*

$$\varphi(x_j, x_i) = (x_j^T x_i + t)^d \quad t \geq 0,$$

where  $2\sigma^2$  is the variance of the Gaussian kernel.

### 2) Data preprocessing

The dataset gathered through the experiments for each noncommercial material was partitioned into two subsets: (1) a training set (70%) to construct the model and (2) a test set (30%) to estimate the performance of the trained model.

Both of the training and testing datasets were normalized to prevent the model from being dominated by the input features with large values. The performance of LS-SVM with scaled (normalized and zero mean) input data has been shown to outperform the same with nonnormalized input data. Scaling is carried out using the following formula:

$$x' = \frac{x - \text{mean}}{\text{standard deviation}},$$

where  $x$  and  $x'$  are the old and the new values of each variable in the dataset, respectively. The LS-SVM model output is denormalized to be transformed back to its original form.

### 3) Performance Measure

The mean absolute error (MAE) and root mean square error (RMSE) criteria were used to measure how close the predicted values by LS-SVM are to the experimental ones. MAE and RMSE are defined by the following equations:

$$MAE = \frac{1}{n} \sum_{i=1}^n |f_i - y_i| = \frac{1}{n} \sum_{i=1}^n |e_i|,$$

$$RMSE = \sqrt{\frac{1}{n} \sum_{i=1}^n (f_i - y_i)^2},$$

where  $f_i$  and  $y_i$  are the predicted and experimental values, respectively.

### 4) LS-SVM hyperparameter selection

LS-SVM hyperparameters are the regularization parameter  $\gamma$  and the kernel parameters ( $\sigma^2$  for the RBF kernel and  $t, d$  for the polynomial kernel). The selection of these parameters plays a crucial role in the performance of the LS-SVM regression models. The regularization parameter  $\gamma$  is critical as it determines the trade-off between the fitting error minimization and smoothness of the estimated function. It is not known beforehand which values are the best for a particular problem to achieve the maximum performance with LS-SVM models. A methodology should be adopted to search in the hyperparameter space during the development period of regression models. This research adopts  $L$ -fold cross-validation (CV), coupled simulated annealing (CSA) [30], and Nelder–Mead simplex algorithms [21] for this purpose.

#### a) L-Fold CV

The training dataset  $D$  is permuted randomly and then partitioned into  $L$  disjoint subsets almost equal in size ( $D_1, D_2, \dots, D_i, \dots, D_L$ ). At the iteration  $i$ , the subset  $i$  is used in testing or validating the model trained using the rest ( $L - 1$ ) of the subsets. The training and validating

process is continued until each subset is used for validation once. Consequently,  $L$  candidate LS-SVMs are obtained and the best of them is selected. The mean of the performance assessments of the  $L$  obtained LS-SVMs is called CV performance or CV error and is used as a predictor of the performance of the LS-SVM model when verified by  $D$ . To select the suitable hyperparameters using  $L$ -fold CV, the CV error is computed for different values of hybrid parameters, and then the model with the lowest CV error is selected and trained using the whole training dataset.

#### b) Hyperparameters initialization and tuning

The initialization and search in the parameter space are performed using CSA for global optimization and simplex algorithms for local optimization. Firstly, the CSA determines the suitable parameters according to some criterion. Then, these parameters are fine-tuned using Nelder–Mead simplex. The CSA has a better optimization efficiency than multistart simulated annealing [30]. Moreover, the CSA is less sensitive to the initialization parameters.

## III. RESULTS AND DISCUSSION

Two independent LS-SVM models were trained: one to predict the friction force in newton (N) and the other to predict the temperature using the dataset for material NF1 under different braking conditions; we called them F-LS-SVM and T-LS-SVM. RBF and polynomial kernels were adopted. LS-SVM Lib. v.1.8 [7] was used for the purpose of training and testing the models.

### A. RBF Kernel Based Models

F-LS-SVM and T-LS-SVM were developed using RBF kernels. Tables III and IV list the hyperparameters of the best seven F-LS-SVM and seven T-LS-SVM models resulting from applying threefold to tenfold CV. Each of these models was trained using the training dataset and then tested twice, once using the training dataset and then using the testing datasets of NF1. MAE and RMSE were computed for each model and are listed in the tables (where MAE-Te and RMSE-Te are the MAE and RMSE values when verifying the models using the testing data, whereas MAE-Tr and RMSE-Tr are the MAE and RMSE values when verifying the models using the training data). By looking at Table III and comparing the values of MAE-Te and RMSE-Te to the corresponding MAE-Tr and RMSE-Tr, it can be concluded that the performance of each of the seven F-LS-SVMs over the trained data is better than the performance of each model over the testing data, which may indicate that the models suffer from an underfitting problem. The increase in the size of the training dataset will not result in better performance models. While it is obvious from Table IV and Figs. 4 and 5 that some of the trained T-LS-SVM models generalized well, the best of them is the one that resulted from the fivefold CV, where MAE-Te = 1.44, RMSE-Te = 1.93, the difference between MAE-Te and MAE-Tr = 0.33, and

the difference between RMSE-Te and RMSE-Tr = 0.7, which are the minimum compared to the other models.

**B. Polynomial Kernel Based Models**

The training process was repeated again to develop F-LS-SVM and T-LS-SVM models using polynomial kernels. Tables V and VI list the hyperparameters, MAE, and RMSE for each developed F-LS-SVM and T-LS-SVM model. Figures 6–9 visualize the MAE and RMSE when verifying the models using testing and training datasets of NF1. As observed, polynomial kernel based F-LS-SVM models generalized better than RBF based models. The performance of the polynomial kernel F-LS-

SVM, degree three, that resulted from threefold CV is the best (MAE-Te = 0.17, RMSE-Te = 0.35). It is also noted that the performance of the polynomial kernel, degree three, T-LS-SVM model (MAE-Te = 1.42, RMSE-Te = 1.88) is the best among all the polynomial and RBF kernel T-LS-SVM models.

Figs. 10, 12, and 14 show the predicted friction force (using F-LS-SVM, polynomial kernel, degree three) against the measured ones at different values of load, speed, and duration. Figs. 11, 13, and 15 show the predicted temperature (using T-LS-SVM, polynomial kernel, degree three) against the measured ones at different values of load, speed, and duration.

TABLE III. TRAINED F-LS-SVM TO MODEL NF1, RBF KERNEL, USING THREEFOLD TO TENFOLD CV.

		L-fold CV							
		3-fold	4-fold	5-fold	6-fold	7-fold	8-fold	9-fold	10-fold
F-LS-SVM model	$\gamma$	1026	1000	35074488	122177	8106	4275632	37713	13871
	$\sigma^2$	0.151	0.136	0.195	0.083	0.065	0.138	0.088	0.047
Performance evaluation (MAE, RMSE)	MAE-Te	0.995	1.002	13.494	1.697	1.060	5.352	1.352	1.083
	MAE-Tr	0.040	0.039	0.016	0.016	0.019	0.016	0.019	0.015
	RMSE-Te	1.42	1.43	28.44	2.42	1.53	8.89	1.98	1.54
	RMSE-Tr	0.11	0.11	0.03	0.03	0.05	0.03	0.04	0.03

TABLE IV. TRAINED T-LS-SVM TO MODEL NF1, RBF KERNEL, USING THREEFOLD TO TENFOLD CV.

		L-fold CV							
		3-fold	4-fold	5-fold	6-fold	7-fold	8-fold	9-fold	10-fold
T-LS-SVM model	$\gamma$	397	106	480	624	532	1773	374	2054
	$\sigma^2$	1.72	1.90	0.79	0.46	0.57	0.96	0.52	1.28
Performance evaluation (MAE, RMSE)	MAE-Te	1.81	1.69	1.44	3.63	2.53	1.50	2.79	1.74
	MAE-Tr	1.22	1.32	1.11	1.05	1.08	1.11	1.08	1.15
	RMSE-Te	2.59	2.33	1.93	5.54	3.70	2.06	4.14	2.36
	RMSE-Tr	2.93	3.20	2.63	2.49	2.54	2.62	2.53	2.74

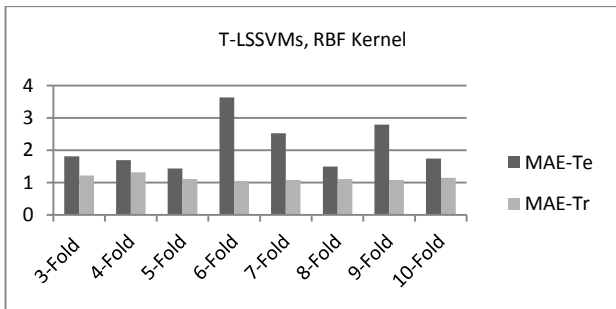


Figure 4. MAE when verifying T-LS-SVM (RBF kernel) models using training and testing datasets of NF1.

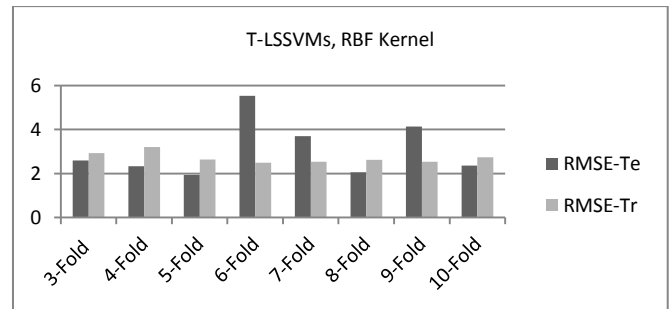


Figure 5. RMSE when verifying T-LS-SVM (RBF kernel) models using training and testing datasets of NF1.

TABLE V. TRAINED F-LS-SVM TO MODEL NF1, POLYNOMIAL KERNEL, USING THREEFOLD TO TENFOLD CV.

		L-fold CV							
		3-fold	4-fold	5-fold	6-fold	7-fold	8-fold	9-fold	10-fold
F-LS-SVM model	$\gamma$	2.634	0.281	2384.588	0.003	4.565	140.093	13.097	1379.124
	$t$	7.86	31.35	11.97	2.16	24.97	5.38	13.78	3.30
	$d$	4	6	5	3	6	4	7	4
Performance evaluation (MAE, RMSE)	MAE-Te	0.17	0.47	0.23	1.01	0.17	0.28	0.22	0.24
	MAE-Tr	0.18	0.26	0.11	0.95	0.19	0.11	0.17	0.09
	RMSE-Te	0.35	0.63	0.38	1.35	0.37	0.42	0.37	0.38
	RMSE-Tr	0.39	0.51	0.28	1.15	0.44	0.29	0.40	0.24

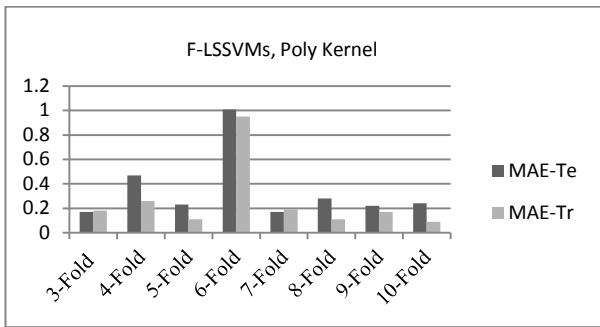


Figure 6. MAE when verifying polynomial F-LS-SVM models using training and testing datasets of NF1.

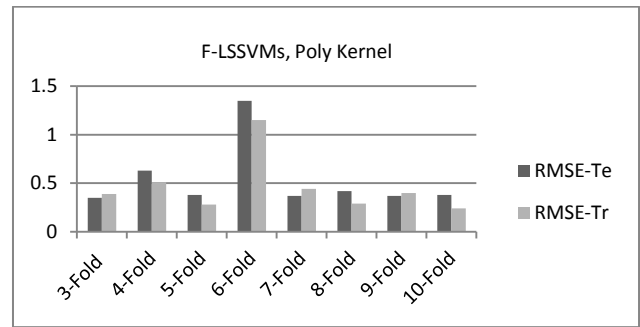


Figure 7. RMSE when verifying polynomial F-LS-SVM models using training and testing datasets of NF1.

TABLE VI. TRAINED T-LS-SVM TO MODEL NF1, POLYNOMIAL KERNEL, USING THREEFOLD TO TENFOLD CV.

		<i>L</i> -fold CV							
		3-fold	4-fold	5-fold	6-fold	7-fold	8-fold	9-fold	10-fold
<b>T-LS-SVM model</b>	$\gamma$	515.96	0.01	0.18	91.38	4.06	0.01	0.29	0.01
	$t$	3.53	61.99	7.86	3.74	6.19	57.74	6.22	13.67
	$d$	4	3	3	5	4	3	5	3
<b>Performance evaluation (MAE, RMSE)</b>	<b>MAE-Te</b>	1.42	11.92	8.75	1.52	1.62	12.13	7.31	11.89
	<b>MAE-Tr</b>	1.41	6.73	3.74	1.55	1.88	7.27	3.20	6.69
	<b>RMSE-Te</b>	1.88	7.87	2.80	1.93	2.49	7.60	2.49	3.70
	<b>RMSE-Tr</b>	2.00	1.73	1.73	2.24	2.00	1.73	2.24	1.73

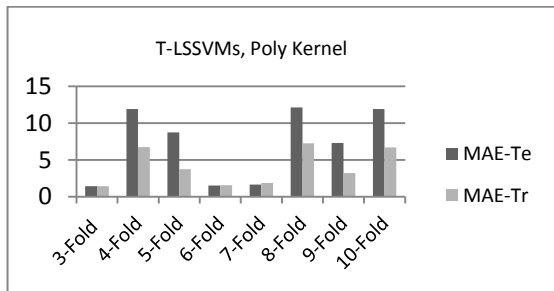


Figure 8. MAE when verifying T-LS-SVM (polynomial kernel) models using training and testing data of NF1.

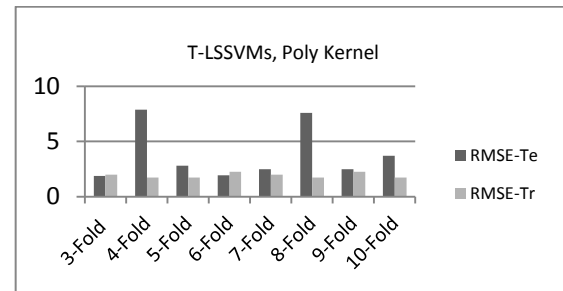


Figure 9. RMSE when verifying T-LS-SVM (polynomial kernel) models using training and testing data of NF1.

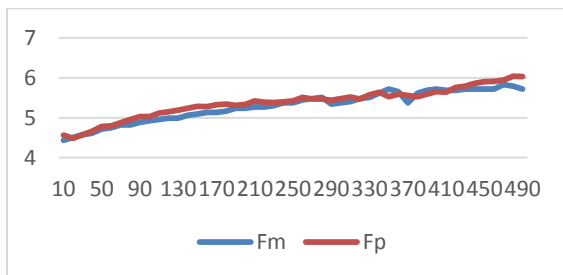


Figure 10. Predicted (Fp) and measured (Fm) friction (N) of NF1 at load = 120 N and speed = 335 m/s.

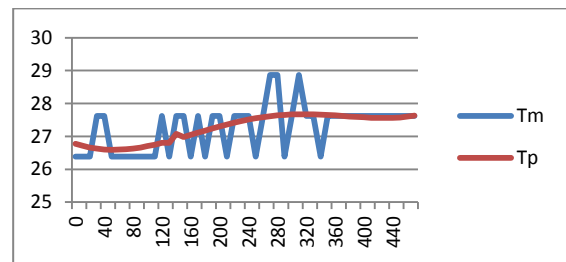


Figure 11. Predicted (Tp) and measured (Tm) interface temperature of NF1 at load = 120 N and speed = 335 m/s.

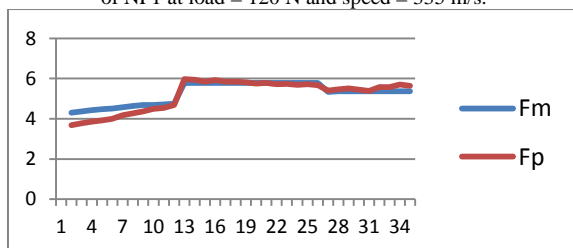


Figure 12. Predicted (Fp) and measured (Fm) friction (N) of NF1 at load = 120 N and speed = 427 m/s.

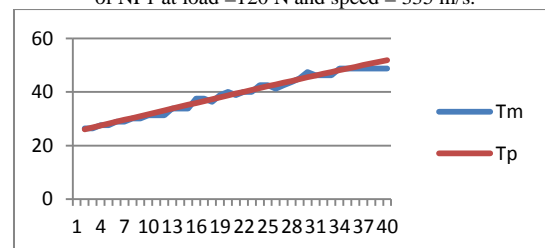


Figure 13. Predicted (Tp) and measured (Tm) interface temperature of NF1 at load = 120 N and speed = 427 m/s.

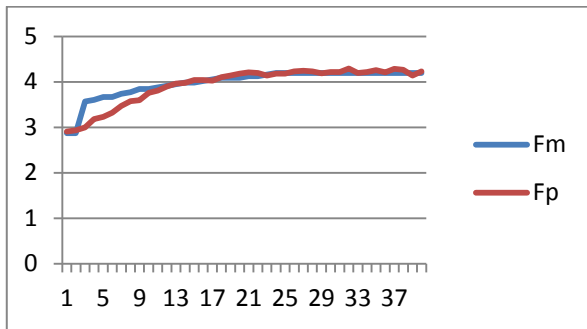


Figure 14. Predicted (Fp) and measured (Fm) friction (N) of NF1 at load = 63 N and speed = 390 m/s.

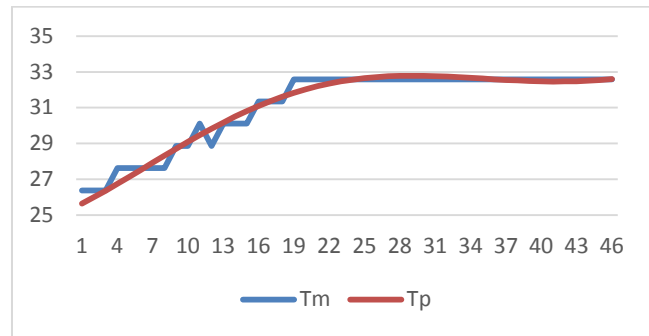


Figure 15. Predicted (Tp) and measured (Tm) interface temperature of NF1 at load = 63 N and speed = 390 m/s.

#### IV. CONCLUSION AND FUTURE WORK

In the field of engineering tribology, very complex and highly nonlinear relationships are involved. This is the reason why analytical models are difficult and machine learning techniques are preferred over other modeling techniques, the reason being their capability in modeling nonlinear behaviors through learning from experimental data and generalization. One of these techniques is LS-SVM, which is a reformulation of the traditional SVM technique where the regression problem is solved by a linear equation system rather than QP, as in SVM.

In this paper, two independent LS-SVM models were developed in order to predict the frictional and thermal behavior of a previously developed noncommercial brake pad material under various pressure and speed conditions.

A set of data was produced experimentally and used in training and testing the LS-SVM models.

LS-SVM models with different kernel functions (RBF and polynomial kernel) were developed. *L*-fold CV, CSA, and Nelder–Mead simplex algorithms were used to select for each model its kernel parameters.

Results showed that some of the models were not able to generalize well, whereas some other models were able to generalize efficiently and predict both of the friction force and the induced temperature. The best performance, in terms of MAE and RMSE, was produced by the models that are based on polynomial kernels, degree three.

As the results are prominent, we are currently working on developing models for the other three noncommercial materials (NF2, NF4 & NF5), in addition to considering more mechanical properties like hardness and density in developing the models.

#### REFERENCES

- [1] D. Aleksendri, D. C. Barton, "Neuro-gentic optimization of disc brake speed sensitivity," *International Journal of Vehicle Design*, vol. 66, no. 3, pp. 258-271, 2014.
- [2] N. Ampazis and N. D. Alexopoulos, "Prediction of aircraft aluminum alloys tensile mechanical properties degradation using support vector machines," *Artificial Intelligence: Theories, Models and Applications Lecture Notes in Computer Science*, vol. 6040, pp. 9-18, 2010.
- [3] O. Abuomar, S. Nouranian, R. King, T. M. Ricks, T. E. Lacy, "Comprehensive mechanical property classification of vapor-grown carbon nanofiber/vinyl ester nanocomposites using support vector machines", *computational material science*, Elsevier, 2015
- [4] A. Besalatpour, M. Hajabbasi, S. Ayoubi, A. Gharipour, A. Jazi1, "Prediction of soil physical properties by optimized support vector machines," *International Agrophysics*, vol. 26, 2012.
- [5] O. Chapelle and V. Vapnik, "Model selection for support vector machines," *Advances in Neural Information Processing Systems* 12, MIT Press, Cambridge, MA, pp. 230-236, 2000.
- [6] O. Chapelle, V. Vapnik, O. Bousquet, and S. Mukherjee, "Choosing multiple parameters for support vector machines," *Machine Learning*, vol. 46, no. 1, pp. 131-159, 2002.
- [7] C. C. Chang and C. J. Lin, *libsvm: a library for support vector machines*, 2001, available: <http://www.csie.ntu.edu.tw/~cjlin/libsvm>
- [8] L. J. Dong, X. B. Li, and Z. L. Zhou, "Nonlinear model-based support vector machine for predicting rock mechanical behaviors," *Advanced Science Letters*, vol. 5, no. 2, pp. 806-810, 2012.
- [9] J. De Brabanter, K. Pelckmans, J. A. K. Suykens, J. Vandewalle, "Robust crossvalidation score function for LS-SVM non-linear function estimation," in *Proc. International Conference on Artificial Neural Networks (ICANN 2002)*, Madrid Spain, Madrid, Spain, pp.713-719, Aug. 2002.
- [10] N. S. M. EL-Tayeb, K. W. Liew, and V. C. Venkatesh, "Evaluation of new frictional brake pad materials," *International Journal of Precision Technology*, vol. 1, No.2 pp. 213 - 222, 2009.
- [11] N. S. M. EL-Tayeb and K. W. Liew, "On the dry and wet sliding performance of potentially new frictional brake pad materials for automotive industry," *Wear* 266, pp. 275-287, 2009.
- [12] C. Fan, Y. He, H. Zhang, H. Li, F. Li, "Predictive model based on genetic algorithm-neural network for fatigue performances of pre-corroded aluminum alloys," *Key Engineering Materials*, pp. 353-358, pp. 1029-1032, 2007.
- [13] C. Fan, Y. He, H. Li, and F. Li, "Performance prediction of pre-corroded aluminum alloy using genetic algorithm-neural network and fuzzy neural network," *Advanced Materials Research*, pp. 1283-1288, 2008.
- [14] S. Fang, M. Wanga, and M. Song, "An approach for the aging process optimization of al-zn-mg-cu series alloys," *Materials and Design* 30, pp. 2460-2467, 2009.
- [15] W. Grzegorzec and S. F. Scieszka, "Prediction on friction characteristics of industrial brakes using artificial neural networks," in *Proc. the Institution of Mechanical Engineers Part J: Journal of Engineering Tribology*, vol. 228, no. 10, pp.1025-1035, 2013.
- [16] Z. Z. Hou, Y. L. Du, M. Zhao, W. G. Zhao, and S. C. Peng, "Application of support vector machine to predicting mechanical properties of tc4", *Advanced Materials Research*, pp. 1854-1857, 2011.
- [17] T. Hastie, R. Tibshirani, and J. Friedman, "The Elements of Statistical Learning", *Springer Series on Statistics*, 2008.
- [18] J. Leifer, "Prediction of aluminum pitting in natural waters via artificial neural network analysis", *Corrosion* 56, pp.563-571, 2000.

- [19] Y. Liu, Q. Zhong, and Z. Zhang, "Predictive model based on artificial neural network for fatigue performance of prior-corroded aluminum alloys", *Acta Aeronautica Et Astronautica Sinica* 22, pp. 135-139, 2001.
- [20] F. F. Martinsa, A. Begonhab, and M. A. S. Braga, "Prediction of the mechanical behaviour of the oporto granite using data mining techniques," *Expert Systems with Applications*, Elsevier, 2012
- [21] J. A. Nelder and R. Mead, "A simplex method for function minimization," *Computer Journal*, 7, pp. 308-313, 1965.
- [22] R. Pidaparti and E. Neblett, "Neural network mapping of corrosion induced chemical elements degradation in aircraft aluminum. Computers," *Materials and Continua* 5, pp. 1-9, 2007.
- [23] N. U. Rathod, V. Seram, and K. Karthik, "Prediction of coefficient of friction and sliding wear rates of cast Al6061-Si3N4 composites using ANN Approach," *International Journal of Scientific Engineering and Research (IJSER)*, vol. 3, no. 2, 2015.
- [24] J. A. K. Suykens, J. De Brabanter, L. Lukas, J. Vandewalle, "Weighted least squares support vector machines: robustness and sparse approximation," *Neurocomputing, Special Issue on Fundamental and Information Processing Aspects of Neurocomputing*, 48(1-4), pp. 85-105, 2002.
- [25] J. A. K. Suykens, J. Vandewalle, and B. De Moor, "Intelligence and cooperative search by coupled local minimizers", *International Journal of Bifurcation and Chaos*, 11(8), 2001.
- [26] J. A. K. Suykens and J. Vandewalle, "Least squares support vector machine classifiers", *Neural Processing Letters*, vol. 9, no. 3, pp.293-300, 1999.
- [27] J. A. K. Suykens, T. Van, De brabanter, B. Demoor, and J. Vandewalle, "Least squares supportvector machines", *World Scientific*, 2002.
- [28] H. Heikh and S. Serajzadeh, "Estimation of flow stress behavior of aa5083 using artificial neural networks with regard to dynamic strain ageing effect", *Journal of Materials Processing Technology* 196, pp. 115-119, 2008.
- [29] V. Vapnik and O. Chapelle, "Bounds on error expectation for support vector machines", *Neural Computation*, vol. 12. no. 9, pp.2013-2036, 2000.
- [30] S. Xavier de Souza, J. A. K. Suykens, J. Vandewalle, and D. Boll é, "Coupled Simulated Annealing", *IEEE Transactions on Systems, Man and Cybernetics - Part B*, vol. 40, no. 2, pp.320-335, 2010.